

Restoration of Enzymatic Activity in a Ser-49 Phospholipase A₂ Homologue Decreases Its Ca²⁺-Independent Membrane-Damaging Activity and Increases Its Toxicity[†]

Toni Petan, Igor Križaj, and Jože Pungercar*

Department of Molecular and Biomedical Sciences, Jožef Stefan Institute, Jamova 39, SI-1000 Ljubljana, Slovenia

Received July 3, 2007; Revised Manuscript Received August 21, 2007

ABSTRACT: Ammodytin L (AtnL) is a Ser-49 secretory phospholipase A₂ (sPLA₂) homologue with myotoxic activity. By analogy to the Lys-49 sPLA₂ myotoxins, AtnL has been predicted to be enzymatically inactive due to the absence of the conserved Asp-49 that participates in coordination of the Ca²⁺ cofactor. By substituting Ser-49 and three other residues in the Ca²⁺-binding loop of AtnL, we obtained the first two enzymatically active mutants of Lys-49/Ser-49 sPLA₂ homologues. The mutants LW and LV, which differed only by the presence of Trp and Val at position 31, respectively, efficiently hydrolyzed phospholipid vesicles, while recombinant AtnL displayed no activity. In contrast to AtnL but similarly to ammodytoxin A (AtxA), a homologous neurotoxic sPLA₂, both mutants exhibited catalysis-dependent membrane-damaging ability, involving vesicle contents leakage and fusion. However, LW and LV also exhibited the potent, Ca²⁺-independent disruption of vesicle integrity characteristic of AtnL, but not of AtxA, in which leakage of the contents is not associated with membrane fusion. Although LV and, especially, LW have the advantage over AtnL of being able to act in both Ca²⁺-independent and Ca²⁺-dependent modes, and display higher cytotoxicity and higher lethal potency, they have a lower Ca²⁺-independent membrane-damaging potency and display reduced specificity in targeting muscle fibers in vitro. Our results indicate that, in evolution, Lys-49 and Ser-49 sPLA₂ myotoxins have lost their Ca²⁺-binding ability and enzymatic activity through subtle changes in the Ca²⁺-binding network without affecting the rest of the catalytic machinery, thereby optimizing their Ca²⁺-independent membrane-damaging ability and myotoxic activity.

Phospholipases A₂ (PLA₂s)¹ are a large group of enzymes that catalyze hydrolysis of the *sn*-2 ester bond of glycerophospholipids (1). The family of secreted phospholipases A₂ (sPLA₂s) consists of relatively small (13–18 kDa) disulfide-rich and Ca²⁺-dependent enzymes that are expressed in a variety of mammalian tissues, but are also major components of some animal venoms (2). Mammalian sPLA₂s are involved in arachidonic acid release from cell membranes and play important roles in inflammation, atherosclerosis, host defense, and cancer, but their exact physiological functions remain to be fully elucidated (3). Snake venom sPLA₂s, whose structure is very similar to that of their mammalian homologues, display a remarkable variety of pharmacological and

toxic activities, including myotoxicity and presynaptic neurotoxicity (2).

Interfacial catalysis by sPLA₂ involves two kinetically and structurally independent steps (4). First, to gain access to their substrate, sPLA₂s have to bind to the lipid/water interface by their interfacial binding surface (IBS), a group of residues located on the relatively flat surface of the molecule surrounding the entrance to the active site. Second, the catalytic reaction occurs after productive binding of a single phospholipid molecule in the active site. The catalytic center of sPLA₂s includes a highly conserved His-48/Asp-99 catalytic dyad and an activated water molecule that acts as a nucleophile during hydrolysis of the *sn*-2 ester bond of the phospholipid (5, 6). During the catalytic turnover cycle, the tetrahedral intermediate is stabilized by a Ca²⁺ ion, which is coordinated by the two carboxylate oxygen atoms of Asp-49, by three main-chain carbonyl oxygen atoms of Tyr-28, Gly-30, and Gly-32 in the Ca²⁺-binding loop, by the *pro*-S oxygen of the *sn*-3 phosphate, and by the oxyanion derived from the *sn*-2 carbonyl oxygen of the phospholipid (5). Besides being essential for the catalytic step, calcium is required for the binding of the substrate phospholipid molecule to the active site, but not for adsorption of sPLA₂s to the membrane (7).

Ammodytin L (AtnL) is a myotoxic structural homologue of group IIA sPLA₂s from *Vipera ammodytes ammodytes* snake venom and is one of the two known Ser-49 sPLA₂

[†] This work was supported by Grant P1-0207 from the Slovenian Ministry of Education, Science and Sport.

* To whom correspondence should be addressed. Phone: +386-1-477-3713. Fax: +386-1-477-3984. E-mail: joze.pungercar@ijs.si.

¹ Abbreviations: Atx, ammodytoxin; Atn, ammodytin; BSA, bovine serum albumin; DLS, dynamic light scattering; FABP, fatty acid-binding protein; FRET, fluorescence resonance energy transfer; IBS, interfacial binding surface; LD₅₀, lethal dose for 50% of the population tested; LDH, lactate dehydrogenase; LV, AtnL-H28Y/L31V/N33G/S49D; LW, AtnL-H28Y/L31W/N33G/S49D; LUV, large unilamellar vesicle; NBD-PE, *N*-(7-nitrobenz-2-oxa-1,3-diazol-4-yl)-1,2-dihexadecanoyl-*sn*-glycero-3-phosphoethanolamine; *N*-Rh-PE, *N*-(lissamine rhodamine B sulfonyl)-1,2-dihexadecanoyl-*sn*-glycero-3-phosphoethanolamine; PA, phosphatidic acid; PC/G/S, phosphatidylcholine/glycerol/serine; PLA₂, phospholipase A₂; POPC/G/S, 1-palmitoyl-2-oleoyl-*sn*-glycero-3-phosphocholine/glycerol/serine; sPLA₂, secreted PLA₂; SPR, surface plasmon resonance.

isoforms (8–10). Like the expanding group of Lys-49 sPLA₂ snake venom myotoxins (11), AtnL has been predicted to be enzymatically inactive due to substitution of the conserved Asp-49 (9), with consequent inability to coordinate the essential Ca²⁺ ion (12, 13). Lys-49 sPLA₂s, as well as the Ser-49-containing AtnL, are very active in inducing myonecrosis in vivo and show a potent Ca²⁺-independent membrane-damaging activity in vitro (11, 14). The myotoxic activity of AtnL was first demonstrated by its ability to affect both directly and indirectly elicited nerve–muscle contractions in guinea-pig hemidiaphragm preparations (15). Additionally, AtnL prevented myoblast fusion and induced massive myonecrosis of myotubes differentiated from the primary cells of neonatal rats (9), induced extensive release of creatine kinase from cultured L-6 myotubes (16), and selectively damaged differentiated *Xenopus laevis* muscle fibers in vivo (17). It has been proposed that the myotoxic and cytolytic activities of AtnL are related to its potent Ca²⁺-independent membrane-disruptive activity, observed on liposomes in vitro (16–19). Although the involvement of a skeletal muscle protein acceptor in the process of sPLA₂-induced myotoxicity cannot be ruled out, a considerable body of evidence has been accumulated indicating that the myotoxic effects of Lys-49 and Ser-49 sPLA₂ homologues are a consequence of direct protein–lipid interaction on the plasma membrane of target muscle cells (11, 14, 18, 20–22). However, while enzymatic activity is necessary for the action of presynaptically neurotoxic venom sPLA₂s (23–26), myotoxic activity can apparently be expressed in the absence of PLA₂ activity (14). Inhibition of enzymatic activity reduced, but did not eliminate, the myotoxic activity of certain enzymatically active myotoxic sPLA₂s (20, 27, 28).

The question as to whether Lys-49 and Ser-49 sPLA₂s possess some low levels of catalytic activity has been a subject of considerable controversy over the past two decades (10, 12, 13, 15, 19, 29–31). Low enzymatic activity has been detected in Ser-49 and Lys-49 sPLA₂s in a number of in vitro studies on artificial and natural phospholipid substrates (10, 15, 19, 29, 30). However, all these studies involved toxins isolated from snake venom, and even trace amounts of copurified Asp-49 sPLA₂s could account for the low levels of activity observed (9, 11, 32). In support of the lack of enzymatic activity of Lys-49 sPLA₂s, the molecular structure indicates that the ϵ -amino group of Lys-49 cannot support catalysis, although it is located in the position usually occupied by Ca²⁺ in Asp-49 sPLA₂s (13, 33). Site-directed mutagenesis and inhibition studies have indicated that Asp-49 is indispensable for effective sPLA₂ catalysis (12, 34). The fact that recombinant myotoxic Lys-49 sPLA₂, both ropstoxin I, showed no activity, in contrast to its isolated natural form, strongly supports the proposed lack of catalytic activity of Lys-49 sPLA₂s (31).

Nevertheless, a number of structural studies have indicated that Lys-49 sPLA₂s are able to bind fatty acids and other long-chain ligands in their “active site” (35–39). Moreover, a direct structural connection between ligand binding in the phospholipase active site and conformational changes in the C-terminal “myotoxic site” of Lys-49 sPLA₂s has been proposed (37, 40), providing an attractive explanation for the intriguing conservation of the Asp-49 sPLA₂ catalytic network in these inactive sPLA₂ homologues (13, 33).

However, binding of a phospholipid molecule in the active site of Lys-49 sPLA₂s has not so far been demonstrated, and it is not clear whether fatty acid or phospholipid binding occurs or whether it is relevant to their mechanism of action on target membranes in vivo (37).

In this study we describe the preparation of two enzymatically active mutants of AtnL. To our knowledge, this is the first example of restoration of activity in a Ser-49/Lys-49 sPLA₂ homologue. The relatively small number of substitutions involved indicates that, apart from the residues involved in Ca²⁺ coordination, the remainder of the substrate-binding and catalytic network of AtnL is very well conserved, allowing us to identify the residues that are responsible for the inactivity of the Ser-49/Lys-49 sPLA₂ homologues. Additionally, by preparing recombinant AtnL, we confirmed experimentally the predicted lack of enzymatic activity in this Ser-49 sPLA₂, leading to examination of some of the previously reported properties. Comparison of the interfacial binding and kinetic properties and the membrane-damaging and toxic activities of AtnL and its mutants with those of the closely similar ammodytoxin A (AtxA), which is a potent presynaptic neurotoxin and highly efficient sPLA₂ enzyme, enabled the mechanisms of membrane damage induced by Ser-49/Lys-49 sPLA₂ myotoxins, active Asp-49 myotoxins, and nonmyotoxic Asp-49 sPLA₂ enzymes to be distinguished.

EXPERIMENTAL PROCEDURES

Materials. AtnL and AtnI₂ were purified from *V. ammodytes ammodytes* venom as described (15, 41). The expression plasmid encoding rat liver fatty acid-binding protein (FABP) was provided by Dr. David C. Wilton (University of Southampton, U.K.), and the recombinant protein was prepared as described previously (42). The mouse myoblast C2C12 cell line was provided by Prof. Angelo Poletti (University of Milan, Italy). Restriction endonucleases were obtained from MBI Fermentas and New England Biolabs. T4 polynucleotide kinase and Taq DNA polymerase were from MBI Fermentas and T4 DNA ligase, Vent DNA polymerase, and Taq DNA ligase from New England Biolabs. Oligonucleotides were from MWG-Biotech (Germany). Triton X-100 was from Roche Molecular Biochemicals. POPG, POPS, and POPC were from Avanti Polar Lipids. NBD-PE (*N*-(7-nitrobenz-2-oxa-1,3-diazol-4-yl)-1,2-dihexadecanoyl-*sn*-glycero-3-phosphoethanolamine), *N*-Rh-PE (*N*-(lissamine rhodamine B sulfonyl)-1,2-dihexadecanoyl-*sn*-glycero-3-phosphoethanolamine), 11-dansylundecanoic acid, and 1-palmitoyl-2-pyrenedecanoyl-*sn*-glycero-3-phosphoglycerol were from Invitrogen-Molecular Probes. All other chemicals were of at least analytical grade and were purchased from Sigma and Serva.

Production and Purification of Mutant and Wild-Type Recombinant Proteins. Recombinant AtxA and AtxA-V31W were prepared as described previously (43, 44). The expression plasmid for AtnL was constructed on the basis of a variant of the pT7-7 vector prepared for expression of a nontoxic AtxA fusion protein (43). The AtnL cDNA (8) was amplified by PCR using a sense oligonucleotide primer, 5'-GGATCCATCGAAGGTCGTAGCGTGATCGAATTTGGGAAG-3', which contained the first eight codons of the cDNA sequence for mature AtnL, a *Bam*HI restriction site, and the last six codons of the fusion peptide sequence present

in the modified pT7-7 vector, and an antisense oligonucleotide primer, 5'-AAGCTTTTAGCATTCTCTGAAAC-CCCCTTGC-3', which was complementary to the 3'-end of AtnL cDNA and contained a *Hind*III restriction site. The amplified fragment was inserted into the modified pT7-7 vector, and the resulting AtnL expression vector was used as a template for preparing expression plasmids encoding AtnL-H28Y/L31V/N33G/S49D and AtnL-H28Y/L31W/N33G/S49D mutants (referred to as LV and LW, respectively, throughout the paper) by site-directed mutagenesis using PCR as previously described (45). In the first round of mutagenesis, the S49D mutation was introduced using the mutagenic oligonucleotide 5'-CGTGCATGATTGCTGT-TACGCG-3', while the mutations H28Y/L31V/N33G and H28Y/L31W/N33G were introduced in two separate reactions in the second round of mutagenesis using the oligonucleotides 5'-ATGCTATTGCGGCGTTGGTGGTAAAGG-3' (LV) and 5'-ATGCTATTGCGGCTGGGGTGGTAAAGG-3' (LW). A silent mutation in Gly-32 (GGG → GGT) was introduced to lower the T_m of the oligonucleotides. The sequences of the expression plasmids encoding for AtnL and its mutants were confirmed by nucleotide sequencing. The T7 RNA polymerase-based expression plasmids encoding AtnL, LV, and LW were used to express the recombinant proteins in *Escherichia coli* strain BL21(DE3) (Novagen) as described for AtxA (43). Proteins in the isolated inclusion bodies were S-sulfonated, refolded, activated by trypsin, and purified as described previously (43, 45).

Analytical Methods. Electrospray ionization mass spectrometry (ESI-MS) analysis of the proteins was performed using a high-resolution magnetic-sensor AutospecQ mass spectrometer (Micromass, U.K.). N-terminal sequencing was performed on an Applied Biosystems Procise 492A protein sequencing system. SDS-PAGE was performed on a Mini Protean III system (Bio-Rad) in the presence of 150 mM dithiothreitol on 15% (w/v) polyacrylamide gels, with Coomassie Brilliant Blue R250 staining. The enzymatic activity of sPLA₂s was assayed using a sensitive fluorometric sPLA₂ assay (46) with sonicated vesicles composed of 1-palmitoyl-2-pyrenedecanoyl-*sn*-glycero-3-phosphoglycerol (Invitrogen) on a Safire² microplate detection system (Tecan, Switzerland).

Preparation of Phospholipid Vesicles. Phospholipid stock solutions in chloroform or 2:1 (v/v) chloroform/methanol were stored at -80 °C under an argon atmosphere. Large unilamellar vesicles (LUVs) containing different molar ratios (expressed as percentages throughout the paper) of POPC, POPS, and POPG, with or without the fluorescent probes NBD-PE and *N*-Rh-PE, were prepared by evaporation of a mixture of the lipids in an organic solvent. After all traces of solvent were removed, the dried phospholipids were hydrated with the appropriate buffer above the phase transition temperature and subjected to eight freeze/thaw cycles, and large unilamellar vesicles were prepared by extrusion through a 100 nm polycarbonate membrane using the Lipofast Basic extruder (Avestin, Canada).

Interfacial Kinetic Studies with Phospholipid Vesicles. The enzymatic activity of sPLA₂s was determined on LUVs containing POPC, POPS, POPG, 10% POPS/POPC, or 30% POPS/POPC. The initial rate of hydrolysis of phospholipid vesicles by sPLA₂s was measured by monitoring the displacement of a fluorescent fatty acid analogue from FABP

(47). Assay solutions with a final volume of 1.3 mL were prepared in Hank's balanced salt solution (HBSS) with 1.26 mM Ca²⁺ and 0.9 mM Mg²⁺ (Gibco) and contained 30 μM phospholipid, 1 μM 11-dansylundecanoic acid, and 10 μg of recombinant FABP (47). Assays were performed in acrylic fluorometric cuvettes at 37 °C with magnetic stirring, using a Perkin-Elmer LS50B fluorimeter. Excitation was set at 350 nm and emission at 500 nm, with 10 nm slit widths. All dilutions of sPLA₂s were prepared in assay buffer containing 1 mg/mL fatty acid-free bovine serum albumin (BSA; Sigma) to prevent loss of enzyme due to adsorption to the walls of the tube. Reactions were started by adding 0.5–2000 ng of sPLA₂ (typically 1–2 μL), and the initial (typically 10 s) linear part of the curve was used to calculate the enzymatic activity. Assays were calibrated by adding a methanol solution of oleic acid (200 pmol/μL) and monitoring the decrease in fluorescence.

Release of Encapsulated Fluorescent Marker from Phospholipid Vesicles. Calcein-loaded LUVs composed of POPC, 10% POPG/POPC, and 50% POPG/POPC were prepared by extrusion as described above. The hydration buffer was composed of 60 mM calcein in either HBSS with 1.26 mM Ca²⁺ and 0.9 mM Mg²⁺ or HBSS without Ca²⁺ and Mg²⁺, 1 mM EGTA, pH 8.0. Vesicles were separated from nonencapsulated calcein by gel filtration on a Sephadex G-25 column. The total phospholipid concentration was determined using the Phospholipids B kit (Waco Chemicals, Germany). Assays were performed in 96-well plates in a final volume of 200 μL per well containing 30 μM total phospholipid in HBSS, with or without Ca²⁺. Measurements were started after addition of 1–5 μL of proteins diluted in assay buffer to triplicate wells, and release of calcein was followed as an increase in fluorescence emission measured at 520 nm on a Safire² microplate fluorimeter (Tecan), with excitation at 485 nm. The results are presented as the percentage of maximal vesicle permeabilization, P (%) = $100(F - F_0)/(F_{\max} - F_0)$, where F is the fluorescence intensity at a specific time point after addition of the toxin, F_0 is the fluorescence intensity of the control without toxin, and F_{\max} is the maximal fluorescence value obtained after addition of Triton X-100 (0.15% (v/v) final concentration).

Fluorescence Resonance Energy Transfer (FRET) Assay of Intervesicular Lipid Mixing. Resonance energy transfer between NBD-PE and *N*-Rh-PE was used to monitor membrane fusion (48). Donor vesicles (20 μM final concentration) of 30% or 50% POPG/POPC or 50% POPS/POPC containing 0.3 mol % each of NBD-PE and *N*-Rh-PE were mixed with a 5-fold excess of unlabeled acceptor vesicles in either HBSS with 1.26 mM Ca²⁺ and 0.9 mM Mg²⁺ or HBSS without Ca²⁺ and Mg²⁺, 0.1 mM EGTA. Measurements were started after addition of 1–5 μL of proteins diluted in assay buffer to triplicate wells with a 200 μL final volume; the decrease in rhodamine fluorescence emission was followed at 581 nm on a Safire² microplate fluorimeter (Tecan), with the excitation wavelength set to 463 nm. The drop in fluorescence for each sample at a given time point was calculated as $\delta F = (F_i - F)$, where F_i is the initial fluorescence intensity. Results are presented as the ratio of δF to the difference in fluorescence signal between the negative control and the total probe dilution control containing 0.15% (v/v) Triton X-100.

Dynamic Light Scattering (DLS). DLS measurements with 50% POPG/POPC vesicles were performed at 37 °C using a PDDLs/BatchPlus System (Precision Detectors). Assay solutions with a final volume of 400 μ L containing 30 μ M phospholipid were prepared in either HBSS with 1.26 mM Ca^{2+} and 0.9 mM Mg^{2+} or HBSS without Ca^{2+} and Mg^{2+} , 0.1 mM EGTA. Typically, at least 50 accumulated correlation functions, obtained with a run time of 1 s and sample time set to 10 μ s, were used per measurement to calculate the diameter of scattering particles using the PrecisionDeconvolve software provided by the manufacturer. The stability of the vesicles was confirmed with repeated measurements for at least 10 min before each measurement with the toxins was started.

Surface Plasmon Resonance (SPR) Measurements of Binding to Phospholipid Vesicles. Extruded LUVs of POPG and POPC were prepared after hydration of the dried lipid film (see above) with the SPR flow buffer (HBSS without Ca^{2+} and Mg^{2+} , containing 100 μ M EGTA). Before SPR measurements, the chip surface was conditioned with three consecutive injections of 2:3 (v/v) 2-propanol/50 mM NaOH, and the Biacore X instrument (Biacore AB, Sweden) was allowed to equilibrate with flow buffer. Vesicles were immobilized on a Pioneer L1 sensor chip by passing a suspension of vesicles with a phospholipid concentration of 3 mM over the chip for 10 min at a flow rate of 1 μ L/min (49). The amount of vesicles coated on the chip was dependent on the type of lipid injected; maximal deposition was reached at 6400 RU for POPG and at 9300 RU for POPC vesicles. The sensor chip was washed twice with 60 μ L of 100 mM NaOH at 60 μ L/min to remove unattached vesicles, which typically resulted in a decrease in the SPR signal not higher than 100 RU. To block the exposed sites on the chip surface, 10 μ L of 0.1 mg/mL fatty acid-free BSA was injected at 1 μ L/min at least twice, or until the chip was saturated, typically increasing the signal by approximately 1000 RU. In measurements with POPC vesicles this surface was once again washed with 100 mM NaOH to stabilize the baseline before each measurement. All measurements with POPG vesicles were performed 30 min after the last BSA injection, when the baseline drift was stabilized, since washing with NaOH removed most of the bound BSA. In control experiments, BSA was deposited on the sensor surface in the absence of phospholipid vesicles and effective prevention of nonspecific binding of sPLA₂s to the sensor chip was confirmed. All binding experiments were performed at 24 °C and with a high flow rate of 60 μ L/min to minimize mass transport effects. Association was monitored for 60 s and dissociation for 3 min. In measurements with POPC vesicles the immobilized lipid surface was regenerated between subsequent measurements by injecting 60 μ L of 100 mM NaOH. After each measurement with POPG vesicles, the sensor chip was washed three times with 2:3 (v/v) 2-propanol/50 mM NaOH to remove all of the vesicles and was then recoated with a fresh vesicle suspension for the next measurement.

Release of Lactate Dehydrogenase (LDH) from C2C12 Myoblasts and Myotubes. C2C12 cells were routinely maintained in Dulbecco's modified Eagle's medium (Gibco) supplemented with 20% (v/v) fetal bovine serum (Gibco) and 2 mM glutamine at 37 °C in a humidified atmosphere of 5% CO₂. The LDH cytotoxicity detection kit (Roche),

which is based on quantification of LDH activity released from the cytosol of damaged cells, was used for determination of cytolysis induced by the sPLA₂s and AtnL. Cells were seeded in 96-well plates at 5000 cells/well and allowed to adhere for 24 h, the culture medium was removed, and the cells were treated in triplicate with the proteins diluted in 200 μ L of assay medium (culture medium containing 1% (v/v) fetal bovine serum and no pyruvate). Maximal LDH release was induced using 2% (v/v) Triton X-100 in assay medium. After 24 h, 100 μ L of culture medium was removed from each well and assayed for LDH activity according to the manufacturer's instructions using a Safire² microplate spectrofluorimeter (Tecan). Experiments with C2C12 myotubes were performed following the same procedure except that, prior to the addition of toxins, the cells were allowed to differentiate for 9 days in Dulbecco's modified Eagle's medium supplemented with 2% (v/v) fetal horse serum.

Toxicity. The lethal potency of the toxins was determined by intraperitoneal injection into BALB/c albino mice. Five dose levels and nine mice per dose were used for each toxin. Samples of recombinant toxins (1–250 μ g), dissolved in water, were diluted to a final volume of 0.5 mL in 0.9% (w/v) NaCl just prior to application. The animals were observed after 24 h and LD₅₀ values determined using the standard method (50).

RESULTS

Structural Integrity of Recombinant AtnL and Its Mutants. Recombinant wild-type AtnL and its mutants AtnL-H28Y/L31V/N33G/S49D (LV) and AtnL-H28Y/L31W/N33G/S49D (LW) were successfully prepared using the previously described methods developed for the expression, refolding, and purification of ammodytoxins (Atxs) (43). Protein homogeneity was demonstrated by SDS-PAGE, analytical RP-HPLC, ESI-MS, and N-terminal sequencing. The relative molecular masses determined for recombinant AtnL (13 857), LV (13 840), and LW (13 928) were within 1 mass unit of those expected, indicating proper pairing of disulfide bonds and the absence of post-translational modifications in the recombinant proteins. The expected single N-terminal sequence, SVIEFGK..., was confirmed for all three recombinant ammodytins (Atns), verifying that the fusion peptide was successfully removed and that no internal cleavages had occurred during activation by trypsin. Additional information about the structural integrity of the mutants and the absence of significant conformational changes in the structure due to the mutations was obtained from their enzymatic activity and from the interfacial binding response curves obtained in SPR measurements. LV and LW had similar, relatively high catalytic activities on POPG vesicles, and their binding affinities for the latter were similar to that of AtnL (see below). Additionally, both recombinant and highly purified natural AtnL, isolated from the venom of *V. ammodytes ammodytes*, displayed a very similar efficacy in inducing calcein release (see below), providing further evidence for the proper folding and structural integrity of the recombinant protein.

Enzymatic Activity and Lethal Potency of Recombinant and Natural AtnL. The use of recombinant AtnL for the first time in the present work enabled us to re-examine several of the previously characterized properties of the natural

Table 1: Lethal Potency of AtnL and Its Mutants^a

sPLA ₂	LD ₅₀ (mg/kg)	sPLA ₂	LD ₅₀ (mg/kg)
AtnL _{rec}	> 10	LW	2.2
AtnL _{nat}	3.6 ^b	AtxA	0.021 ^c
LV	> 7		

^a LD₅₀ values are estimated to be accurate to within ± 5 –10%. Abbreviations: AtnL_{rec}, recombinant AtnL; AtnL_{nat}, natural AtnL isolated from *V. ammodytes ammodytes* venom. ^b Reference 15. ^c Reference 45.

protein. Surprisingly, recombinant AtnL was not lethal to mice even at 10 mg/kg, the highest dose used in the study (Table 1). This value is significantly higher than the LD₅₀ value of 3.6 mg/mL previously reported for the natural protein (15). This strongly suggests that, due to the difficulty of chromatographic separation of the highly homologous sPLA₂s found in snake venoms (11), the AtnL isolated by Thouin et al. (15) was contaminated with the neurotoxic and enzymatically active Atxs. Indeed, different preparations of AtnL have been reported to have either very low (15, 19) or no measurable enzymatic activity (18, 51), and contamination with neurotoxic Atxs, Asp-49 sPLA₂s, has been confirmed (9). Using the sensitive fluorescent pyrene enzymatic activity assay and the fatty acid displacement assay described above, we have shown in our laboratory that the enzymatic activity of a number of highly purified samples of natural AtnL would correspond to contamination with up to 1% of the enzymatically active Atxs (data not shown). Therefore, given that AtxA is at least 500-fold more toxic than AtnL, even the presence of such small amounts of the highly neurotoxic AtxA could account for significant levels of toxicity of preparations of AtnL. Using the same methods, no activity could be detected for recombinant AtnL, confirming that the enzymatic activity detected in samples of natural AtnL (9, 15, 19) was indeed a consequence of traces of Asp-49 sPLA₂ contaminants. Very careful and repetitive rounds of purification by RP-HPLC finally led to samples of natural AtnL lacking detectable enzymatic activity. The purity of these apparently contaminant-free samples was confirmed by ESI-MS analysis, and they were used in some of the assays performed in this study for comparison with recombinant AtnL.

Enzymatic Activity and Lethal Potency of the LV and LW Mutants. We have suggested that, besides Ser-49, His-28 and Asn-33 in the Ca²⁺-binding loop of AtnL play an important role in disabling its catalytic machinery (9). In an attempt to restore its enzymatic activity, we therefore substituted His-28, Asn-33, and Ser-49 in AtnL with residues that are highly conserved in Asp-49 sPLA₂s—Tyr-28, Gly-33, and Asp-49. Additionally, Leu-31 was replaced by either Val, which is found at this position in the highly homologous AtxA, or Trp, which has been shown to enhance the interfacial binding affinity of mammalian sPLA₂s (52, 53). Further, the introduction of Trp-31 in AtxA has been shown to dramatically increase its already high enzymatic activity on PC-rich vesicles as well as on plasma membranes of intact cells in vitro (44; Table 2) and would thus enable easier detection of enzymatic activity. Comparison of the amino acid sequence of AtnL with that of AtxA revealed no other substitutions crucial for catalytic activity, including the absolutely conserved His-48, Asp-99, Tyr-52, and Tyr-73.

The putative IBS of AtnL, comprising Val-2, Ile-3, Leu-19, Thr-20, Phe-24, Leu-31, Ser-67, Lys-69, Thr-70, Arg-72, Arg-118, Val-119, Leu-121, and Phe-124, is very similar to that proposed for AtxA (44). Therefore, on the basis of our previous studies (44, 54) and the high level of identity between Atxs and AtnL, we expected that the mutants of AtnL should be able to bind to phospholipid surfaces relatively well (see below). By introducing the aforementioned substitutions in AtnL, we obtained two enzymatically active mutants (see below). This is the first example of successful restoration of PLA₂ activity in a Lys-49/Ser-49 sPLA₂ homologue. Interestingly, with the restoration of enzymatic activity and introduction of Trp-31 in AtnL, the mutant protein exhibits markedly increased toxicity. The LD₅₀ values show that the lethal potency of the LW mutant in vivo was at least 4.5-fold higher than that of recombinant AtnL (Table 1). On the other hand, the LV mutant was not lethal to mice in doses up to 7 mg/kg.

Both enzymatically active mutants of AtnL were particularly effective in hydrolyzing phospholipid vesicles containing anionic phospholipid (Table 2). Their initial rates of hydrolysis determined on pure anionic POPG and POPS vesicles were high and identical within experimental error, indicating that conditions of high-affinity binding apply and that both mutants possess a well-functioning catalytic machinery. Additionally, the enzymatic activities of LV and LW, although 5-fold lower on POPG and 13-fold lower on POPS vesicles than that of AtxA, were relatively high and in the range of that of the mammalian group IIA enzyme, known for its physiologically important high binding affinity for anionic membrane surfaces (55, 56).

On the other hand, the hydrolytic activities of LV and LW differed considerably on zwitterionic POPC vesicles, the Trp mutant being approximately 44-fold more effective than the Val mutant. The initial rate of hydrolysis of POPC vesicles by the LV mutant was very low and could only be estimated (Table 2). The inclusion of 10% anionic POPS phospholipid in POPC vesicles resulted in a dramatic 100-fold increase in the activity of the Val mutant and a more modest, but still very significant, 38-fold increase in the case of the Trp mutant. At 30% anionic POPS in POPC vesicles the activity of the LV mutant almost reached that of the Trp variant, being only approximately 2-fold lower. The apparent rate of hydrolysis displayed by the LV mutant increased 100-fold on raising the concentration of POPS from 10% to 30%, while the increase in the case of the LW mutant was only 10-fold and was similar to the effect of increasing the surface concentration of anionic phospholipids in the membrane on the activity of Atxs (Table 2; 44).

Calcein Release from Phospholipid Vesicles. To determine the membrane-damaging efficacy of Atxs and Atns, we used the classical method based on release of calcein entrapped in phospholipid vesicles (57). Vesicle permeabilization, lysis, fusion, or any other process that leads to leakage of its internal contents results in dilution of the fluorophore and relief of calcein self-quenching, which can be followed as an increase in the fluorescence signal. AtnL was not able to induce calcein release from pure POPC vesicles, even at concentrations as high as 3 μ M and over a time period of 20 min (Table 3). However, at the same concentration the enzymatically active mutants of AtnL were able to release small amounts of calcein. LW, which

Table 2: Apparent Rates of Hydrolysis of Phospholipid Vesicles by sPLA₂s^a

sPLA ₂	apparent rate of hydrolysis [$\mu\text{mol}/(\text{min mg})$]				
	POPG	POPS	POPC	10% POPS/POPC	30% POPS/POPC
LV	225 \pm 35	91 \pm 7	\sim 0.005	0.49 \pm 0.04	43 \pm 2
LW	180 \pm 25	89 \pm 10	0.22 \pm 0.03	8.3 \pm 0.3	96 \pm 5
AtxA ^b	1042 \pm 160	1251 \pm 188	3.8 \pm 0.5	56 \pm 6	450 \pm 21
AtxA-V31W ^b	2102 \pm 88	1964 \pm 154	102 \pm 7	525 \pm 28	1957 \pm 36
AtnI ₂ ^b	1070 \pm 150	57 \pm 5	12.3 \pm 1.7	49 \pm 2	159 \pm 16

^a The rate value for each sPLA₂ is the mean \pm SD of at least five independent measurements. ^b The apparent rates of hydrolysis were determined in our previous study (44).

Table 3: Calcein Release from Phospholipid Vesicles by Atxs and Atns^a

sPLA ₂	calcein release (%)			
	POPC	10% POPG/POPC	50% POPG/POPC	50% POPG/POPC, no Ca ²⁺
AtnL _{nat}	\sim 0 (3 μM)	\sim 0.8	52 \pm 3	35 \pm 2
AtnL _{rec}	\sim 0 (3 μM)	\sim 1.2	60 \pm 3	29 \pm 2
LV	\sim 2 (3 μM)	20 \pm 1	35 \pm 1	24 \pm 2
LW	\sim 8 (3 μM)	25 \pm 1; \sim 0 (no Ca ²⁺)	36 \pm 2	19 \pm 2
AtxA	\sim 8; \sim 28 (3 μM)	37 \pm 1; 23 \pm 1 (20 nM)	\sim 74; 17 \pm 1 (2 nM)	not detected
AtnI ₂	not determined	\sim 36; 16 \pm 1 (20 nM)	\sim 30	not detected
AtxA-V31W	not determined	\sim 55; 35 \pm 2 (20 nM)	\sim 83 (250 nM)	not detected

^a Leakage of the vesicle contents was determined by the calcein release method as described in the Experimental Procedures. The results presented are mean values \pm SD of at least three independent measurements 5 min after addition of 500 nM sPLA₂ (unless otherwise indicated). Abbreviations: AtnL_{rec}, recombinant AtnL; AtnL_{nat}, natural AtnL.

displayed a markedly higher enzymatic activity on POPC vesicles than LV, was also more effective in releasing calcein. AtxA was the most effective of the enzymes tested on these vesicles and induced a detectable calcein release at only 500 nM. The ability of the toxins to induce calcein release from POPC vesicles correlated very well with their rates of hydrolysis of these vesicles (Table 2).

AtxA and the enzymatically active mutants of AtnL were much more effective in releasing calcein from POPC vesicles containing 10% anionic phospholipids. Five minutes after the addition of 500 nM toxins to the vesicle suspension, 37% of the total calcein was released by AtxA, while LW and LV released slightly lower amounts of calcein, 25% and 20%, respectively. On the other hand, AtnL did not elicit any significant release of calcein at 500 nM (\sim 1%). Even at a concentration of 10 μM only a modest increase in the signal, corresponding to about 15% of calcein release, was observed (data not shown), but the characteristic time-dependent rise of fluorescence accompanying calcein release was absent. The ability of nontoxic AtnI₂ to induce calcein release was similar to that of AtxA, while the AtxA-V31W mutant, which displays a 10-fold higher enzymatic activity than AtxA on both 10% POPS/POPC (Table 2) and 10% POPG/POPC vesicles (44), was by far the most effective in calcein release. In the absence of calcium, calcein leakage from 10% POPG/POPC vesicles was not detected for any of the enzymes at concentrations of 500 nM, indicating that enzymatic activity is responsible for their calcein release effect. Clearly, apart from AtnL, the calcein-releasing capability of the enzymatically active sPLA₂s increased considerably in the presence of anionic phospholipids in vesicles.

The incorporation of 50% anionic POPG phospholipids in charge-neutral POPC vesicles caused a marked rise in the calcein-releasing efficiency of all the toxins tested, but the most significant increase was observed for AtnL. Enzymatic

activity and calcein release did not correlate on these vesicles. In contrast to its very low efficiency on 10% POPG/POPC, recombinant AtnL (500 nM) was able to induce 60% of the maximal calcein release in the presence of calcium, but was also remarkably effective in the absence of calcium (Table 3 and Figure 1). In the presence of calcium, 2 nM AtxA released 17% of the entrapped calcein after 5 min, and approximately 74% was released at 500 nM. However, AtxA, AtxA-V31W, and AtnI₂ did not release calcein in the absence of calcium, indicating that their membrane-damaging action on these vesicles is dependent on enzymatic activity. LV and LW were less effective in releasing calcein than either AtnL or AtxA in the presence of calcium, displaying 35% and 36% of the maximal release, respectively (Figure 1A). However, both mutants caused a significant Ca²⁺-independent calcein release, suggesting that, unlike AtxA, they are able to induce membrane damage independently of their enzymatic activity. Additionally, in the absence of calcium the kinetics of calcein release induced by LV and LW were very similar to those of AtnL, showing a time-dependent increase not reaching a plateau over the course of the measurement (Figure 1B). On the other hand, their kinetic curves in the presence of calcium closely resembled those displayed by AtxA, showing an abrupt initial release, but very rapidly reaching a plateau level (Figure 1A). Additionally, while the dose-response curve for AtxA reached a plateau at 100 nM, the calcein release induced by AtnL, LW, and LV increased linearly over the range of concentrations tested (25–1500 nM for AtnL and 25–500 nM for the mutants; data not shown). The double-reciprocal plots indicated that there was no cooperativity in the action of AtnL, LW, and LV, and the time dependence of the effect was evident.

Intervesicular Lipid Mixing Analysis by FRET. The fusogenic activity of Atxs and Atns was estimated by their

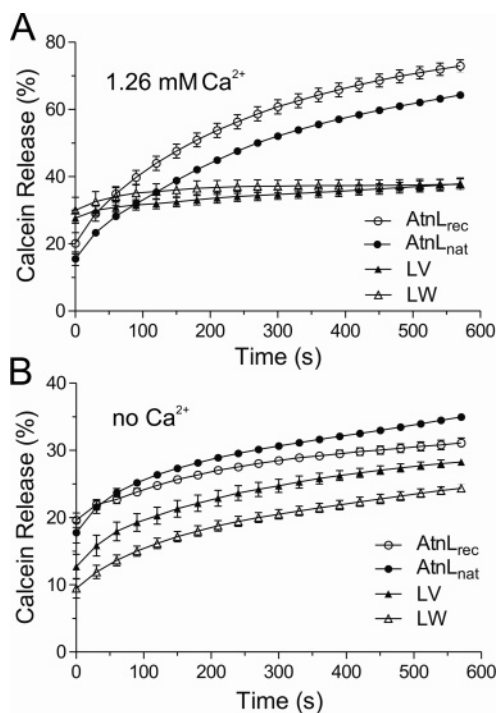


FIGURE 1: Calcein release from 50% POPG/POPC vesicles by AtnL and its mutants in the presence or absence of calcium. Calcein-loaded vesicles composed of 50% POPG/POPC with a total phospholipid concentration of 30 μ M in either HBSS with Ca^{2+} (A) or HBSS without Ca^{2+} , 1 mM EGTA, pH 8.0 (B) were treated with 500 nM recombinant AtnL (○), natural AtnL (●), LV (▲), and LW (△), and the increase in fluorescence emission at 520 nm was followed. The results are presented as a percentage of the maximal fluorescence value obtained after complete vesicle permeabilization with Triton X-100. Error bars are the standard deviations from at least three independent measurements.

ability to induce lipid mixing between two populations of vesicles. When membranes of donor vesicles, labeled with NBD-PE and *N*-Rh-PE, fuse (or semifuse) with unlabeled acceptor vesicles, the average distance between the FRET pair increases, leading to reduction of resonance energy transfer, which can be followed as a decrease in the intensity of rhodamine emission at 581 nm. Using 50% POPG/POPC or 50% POPS/POPC acceptor vesicles, we readily detected lipid mixing with all the enzymes tested, but not with AtnL (Figure 2A). AtxA and its Trp mutant were the most effective, causing 25% and 27% of the total lipid mixing with 50% POPG/POPC vesicles, respectively, but were closely followed by LV, LW, and AtnI₂ (Table 4 and Figure 2B). The ability of all the sPLA₂s to induce lipid mixing was higher when PS-containing acceptor vesicles were used, which is most probably a consequence of facilitated fusion of vesicles composed of different phospholipids. However, in all cases lipid mixing could be detected only in the presence of calcium (data not shown), while the inactive AtnL failed to induce any lipid mixing up to 6.2 μ M, regardless of the absence or presence of up to 5 mM calcium, 1 mM EGTA, or 0.1 mg/mL BSA (Figure 2A). This strongly suggests that the fusogenic activity of the toxins is strictly dependent on their enzymatic activity.

SPR Analysis of Binding to Phospholipid Vesicles. SPR measurements with POPC and POPG vesicles deposited on a Pioneer L1 chip were performed to gain a qualitative assessment of the interfacial binding affinities of AtnL and its mutants compared to those of Atxs (Figure 3). Phos-

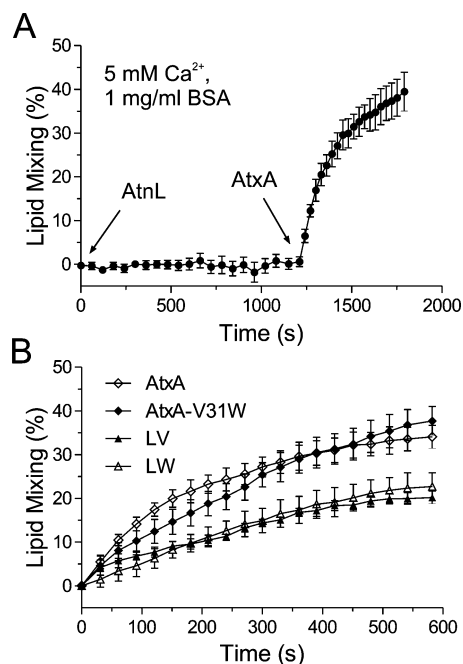


FIGURE 2: Interventric lipid mixing induced by Atxs and Atns. Lipid mixing between NBD-PE/*N*-Rh-PE-labeled donor 50% POPG/POPC vesicles (20 μ M phospholipid) containing a 0.3 mol % concentration of each fluorophore and a 5-fold excess of unlabeled acceptor 50% POPG/POPC vesicles was followed as a decrease in rhodamine fluorescence emission. (A) A 500 nM concentration of recombinant AtnL failed to induce any lipid mixing over a time period of 20 min in HBSS containing 5 mM Ca^{2+} and 1 mg/mL BSA. Lipid mixing could be readily detected after subsequent addition of 500 nM AtxA to the same wells. (B) Interventric lipid mixing induced by 500 nM AtxA (◇), AtxA-V31W (◆), LV (▲), and LW (△) in HBSS with 1.26 mM Ca^{2+} . Error bars represent the standard deviation from at least three independent measurements.

pholipid hydrolysis by sPLA₂s during binding experiments was prevented by omitting Ca^{2+} from the SPR flow buffer. A number of consecutive measurements were routinely made with one deposition of POPC vesicles, since the ligand surface could be effectively and reproducibly regenerated by removing the bound protein with 100 mM NaOH (58), indicating that the toxins did not have a perturbing effect on the vesicles. On the contrary, POPG vesicles had to be freshly deposited before each measurement, since regeneration of the surface following measurements with AtnL and its mutants was not always successful, indicating simultaneous removal of the bound toxin, BSA, and some of the immobilized lipid. This was confirmed when regeneration of the POPG surface was attempted after measurements with high concentrations (i.e., 500 nM) of AtnL, which resulted in a considerable drop of the baseline (\sim 1000 RU below the signal of the deposited lipids; data not shown). The latter effect was not observed either on POPC vesicles with any of the toxins or on POPG vesicles during repetitive measurements with up to 2.4 μ M AtxA. This is an indication of a Ca^{2+} -independent membrane-damaging mechanism of AtnL and its mutants that is related to the presence of anionic phospholipids in the membrane and includes a significant disruption of the bilayer structure.

The interfacial binding experiments performed by SPR indicate that Atns bind very well to zwitterionic POPC and to anionic POPG vesicles. In both cases their apparent

Table 4: Intervesicle Lipid Mixing Induced by Atxs and Atns^a

sPLA ₂	lipid mixing (%)		sPLA ₂	lipid mixing (%)	
	50% POPG/POPC	50% POPS/POPC		50% POPG/POPC	50% POPS/POPC
AtnL _{nat}	not detected	not detected	AtxA	27 ± 2	45 ± 4
AtnL _{rec}	not detected	not detected	AtnI ₂	14 ± 5	18 ± 3
LV	17 ± 1	34 ± 6	AtxA-V31W	25 ± 3	not determined
LW	13 ± 3	38 ± 2			

^a Intervesicle lipid mixing was assayed using 20 μM labeled vesicles of NBD-PE/*N*-Rh-PE/POPG/POPC (0.3%/0.3%/49.7%/49.7%) and 100 μM unlabeled acceptor vesicles, whose compositions are stated in the table. Measurements were performed in triplicate in wells containing 500 nM protein in HBSS as described in the Experimental Procedures. The results are presented as percentages of maximal lipid mixing induced by solubilization of vesicles with Triton X-100, measured 5 min after addition of the protein. The presented value for each protein is the mean ± SD of three independent measurements. See the text for more information.

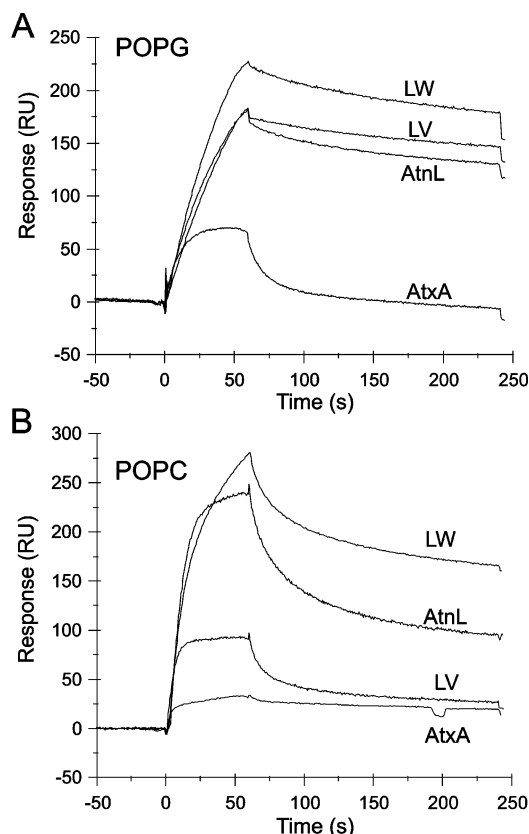


FIGURE 3: Representative sensograms of sPLA₂ binding to immobilized phospholipid vesicles. Large unilamellar vesicles of POPG and POPC prepared in HBSS without Ca²⁺ and Mg²⁺, containing 100 μM EGTA, were immobilized on a Pioneer L1 sensor chip, and nonspecific binding sites were saturated with fatty acid-free BSA as described in the Experimental Procedures. A 50 nM (A) or 100 nM (B) concentration of AtxA, AtnL, LW, or LV was injected over the immobilized POPG (A) or POPC (B) vesicles, and the subsequent association was monitored for 60 s and dissociation for 3 min.

binding affinities were markedly higher than those of AtxA (Figure 3). The maximal relative responses obtained indicate that the LW mutant has the highest affinity for binding to both types of vesicles. The shapes of the binding curves obtained on POPC vesicles suggest that LW has a faster association rate and a slower dissociation rate than the rest of the sPLA₂s. Interestingly, the relative binding response of AtnL was in the same range as that of the LW mutant on POPC vesicles, but the LV mutant displayed a 3-fold lower affinity for zwitterionic vesicles, although its affinity was still approximately 3-fold higher than that of AtxA. This is in accordance with the very significant difference in enzy-

matic activity of the LW and LV mutants on POPC vesicles. The SPR binding responses obtained on POPG vesicles, in which electrostatic forces are likely to dominate in the protein–membrane interactions, indicate that AtnL and its mutants have very similar interfacial binding affinities, while the somewhat less basic AtxA displayed a 2–3-fold lower binding response. Additionally, the lower affinity of AtxA is evident from the shape of its binding curve, especially from the dissociation rate that is markedly higher than that of Atns.

Effects on Vesicle Structural Integrity Studied by Dynamic Light Scattering. DLS was used to determine the size distribution and stability of vesicles used in this study, as well as to analyze the effects of Atxs and Atns on 50% POPG/POPC vesicles. Selected representative measurements are presented in Figure 4. AtxA did not cause any notable changes in vesicle size in the absence of calcium (not shown). The average diameter of 50% POPG/POPC vesicles in a typical measurement was approximately 90 nm (with individual particle diameters ranging from 70 to 130 nm) and remained constant (within 10 nm) during a 15 min measurement with AtxA. On the other hand, regardless of the presence or absence of calcium, the addition of 500 nM AtnL caused the transient appearance of a population of particles with average diameters ranging typically from 160 to 190 nm, most probably indicating association of vesicles into dimeric structures. After prolonged incubation with AtnL (up to 30 min), the majority of phospholipid structures displayed average diameters in the range close to the original vesicle size (100–150 nm), but some small amounts of larger particles with diameters reaching the micrometer range could be detected (Figure 4).

The effects of LW in the absence of calcium were similar to those of AtnL, with the majority of particles retaining a size similar to that of the original vesicles, but in the presence of calcium LW acted in a manner similar to that of AtxA (Figure 4). Incubation of 50% POPG/POPC vesicles with AtxA or LW in the presence of calcium resulted in the rapid appearance of phospholipid structures larger than the original vesicles and with a very wide range of diameters, probably reflecting vesicle aggregation and concomitant fusion. This resulted in a clear bimodal distribution after prolonged incubation, with approximately half the phospholipid structures displaying average diameters ranging from 600 to 800 nm, while the average diameters of the other half were similar to or smaller than those of the original vesicles (60–80 nm). A significant increase of light scattering intensity, an indication of profound alterations in vesicle structure, was

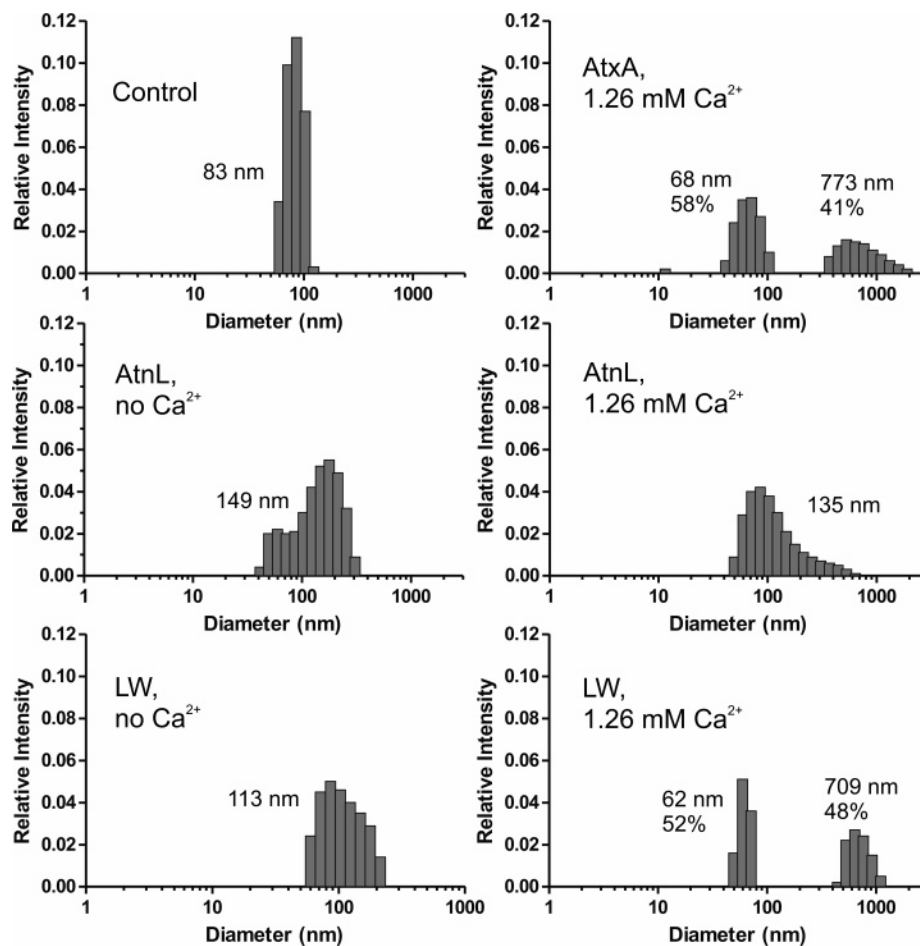


FIGURE 4: Effects of AtxA, AtnL, and LW on the structural integrity of 50% POPG/POPC vesicles. Dynamic light scattering measurements with 50% POPG/POPC vesicles (30 μ M total phospholipid concentration) and 500 nM toxins were performed at 37 $^{\circ}$ C in either HBSS with 1.26 mM Ca^{2+} or HBSS without Ca^{2+} , 0.1 mM EGTA. Representative size distribution plots obtained 15 min after addition of the proteins are shown. The control (upper left panel) contained only 50% POPG/POPC vesicles in HBSS containing 1.26 mM Ca^{2+} . In each panel the average diameter and the percentage of separate population groups are shown.

observed during experiments with AtxA and LW in the presence of calcium, but not in its absence or in measurements with AtnL. Clearly, in the absence of calcium LW affects vesicle structure and integrity in a manner closely resembling that of AtnL, while in the presence of calcium, effects similar to that of AtxA, which are most probably dependent on enzymatic activity, are dominant.

Cytotoxicity. The cytotoxic potency of Atxs and Atns was determined on the basis of LDH release from the cytosol of damaged C2C12 myoblasts or differentiated myotubes. The murine skeletal muscle C2C12 cell line has been used in a number of studies with Lys-49 sPLA₂ myotoxins and has been found to be a suitable *in vitro* model for assessing their membrane-damaging and myotoxic activities (11, 59, 60). A prolonged toxin exposure time of 24 h was chosen in this study to increase the sensitivity of the assay and save valuable amounts of recombinant proteins by allowing the detection of both the rapid cytolytic and the slower apoptotic processes occurring at lower toxin concentrations (14, 61). AtnL exhibited a weak potency in damaging undifferentiated C2C12 myoblasts (Table 5). A 24 h incubation with 500 and 1000 nM concentrations of AtnL resulted in 8% and 12% of the maximal LDH release from C2C12 myoblasts, respectively. The potency of AtnL was thus similar to that of the nontoxic, but enzymatically active, AtnI₂. On the other hand, the enzymatically active LV, and especially LW,

displayed a higher cytotoxicity on C2C12 myoblasts. At 500 nM, LW was 3.8-fold more potent than AtnL, while LV was twice as potent as AtnL at 1000 nM. AtxA displayed the highest cytotoxicity toward C2C12 myoblasts of all the sPLA₂s tested and induced 44% of the maximal LDH release at 500 nM. The cytotoxicity of the tested toxins, which are all basic molecules, correlated well with their enzymatic activity on PC-rich vesicles. The nontoxic AtnI₂ was an exception, since, despite its high enzymatic activity on PC-rich vesicles and its effective calcein release from 10% POPG/POPC vesicles, it displayed the lowest cytotoxicity on C2C12 myoblasts. However, we have shown previously that AtnI₂ has an unusually low enzymatic activity when tested on plasma membranes of intact mammalian cells, while the activities of Atxs on PC vesicles and plasma membranes correlated very well (44).

Differentiated C2C12 cells were much more susceptible to the actions of both Atxs and Atns (Table 5). AtnL showed almost 6-fold higher cytotoxic potency on myotubes than on myoblasts, but its enzymatically active mutants were even more potent. In fact, the cytotoxicity of the LW mutant was higher than that of AtxA and AtxA-V31W, despite the very high enzymatic activity of the latter on PC-rich vesicles, as well as on intact plasma membranes (44). The extent of cytotoxicity induced by the LV mutant was similar to that by AtxA, AtxA-V31W, and AtnI₂. There was no correlation

Table 5: Cytotoxicity of Atxs and Atns on C2C12 Myoblasts and Myotubes^a

sPLA ₂	cytotoxicity (%) on C2C12 myoblasts			cytotoxicity (%) on C2C12 myotubes		
	250 nM	500 nM	1000 nM	250 nM	500 nM	1000 nM
AtnL _{rec}	nd	8 ± 2	12 ± 3	nd	44 ± 23	65 ± 22
LV	nd	11 ± 2	24 ± 8	nd	64 ± 21	83 ± 23
LW	nd	30 ± 6	38 ± 7	nd	88 ± 22	92 ± 22
AtxA	25 ± 8	44 ± 9	nd	44 ± 22	72 ± 30	nd
AtxA-V31W	nd	nd	nd	72 ± 18	73 ± 22	nd
AtnL ₂	6 ± 2	7 ± 2	nd	60 ± 14	61 ± 19	nd

^a The cytotoxicity of Atxs and Atns was estimated by determining the amount of LDH released from C2C12 myoblasts or differentiated myotubes after a 24 h incubation of 5000 cells/well with 250, 500, or 1000 nM toxins. The assays were performed in triplicate, and the values obtained were corrected for background absorbance of the assay medium. Spontaneous release of LDH in the negative control was used to set the cytotoxicity scale to 0, and maximal LDH release was induced using 2% (v/v) Triton X-100 in the assay medium. The values presented are means ± SD of three independent experiments. Abbreviations: AtnL_{rec}, recombinant AtnL; nd, not determined.

between the enzymatic activities of Atxs and Atns on PC-rich membranes and their ability to cause cytolysis of differentiated C2C12 myotubes.

DISCUSSION

Ser-49 sPLA₂ Homologues Are Enzymatically Inactive.

The lack of enzymatic activity in the first recombinant Ser-49 sPLA₂, AtnL, confirms the hypothesis (9) that Ser-49 sPLA₂ homologues are incapable of phospholipid hydrolysis. Our results, together with the recently confirmed inactivity of recombinant bothropstoxin I (31), a Lys-49 sPLA₂ homologue, provide a strong argument in favor of the long-debated lack of phospholipolytic activity of both Ser-49 and Lys-49 sPLA₂ homologues (11). Additionally, our previous suggestion (9) is confirmed, in that the substitution of several conserved residues in Lys-49/Ser-49 sPLA₂ homologues, and not only the essential Asp-49, is responsible for their impaired binding of the calcium cofactor and the resulting lack of enzymatic activity. Similar conclusions were drawn after the preparation of the K49D mutant of bothropstoxin I, where the completion of the catalytic motif His-48/Asp-49/Asp-99 did not result in restoring enzymatic activity (31). The authors suggested that other structural factors, such as the presence of Asn-28 and Leu-31 in the Ca²⁺-binding loop of bothropstoxin I, may be responsible for the loss of its catalytic function. Indeed, the absolutely conserved Tyr-28, which coordinates the Ca²⁺ ion through its carbonyl oxygen in active sPLA₂s, is replaced by Asn in almost all known Lys-49 sPLA₂s (62), by His-28 in AtnL, and by Phe in ecarpholin S, the only Ser-49 sPLA₂ besides AtnL known to date (10). Additionally, two consecutive glycines at positions 32 and 33 are highly conserved in the sPLA₂ family, but are frequently replaced in Lys-49 sPLA₂s (62). In AtnL and ecarpholin S, Asn and Glu, respectively, are present at position 33. The enzymatic activity reported for ecarpholin S (10) appears to be highly unlikely in light of the lack of activity of both recombinant AtnL and bothropstoxin I (31), especially keeping in mind the possibility of contamination of the purified protein with catalytically active sPLA₂s. The fact that the high level of enzymatic activity reported was determined on PC substrates and that it was in the range of the human group IIA enzyme, which in fact displays a very low activity on PC-rich substrates (56), casts further doubt on the reported activity of ecarpholin S. Therefore, our results confirm the hypothesis that, apart from the absence of Asp-49, the frequent and unique substitutions in the Ca²⁺-binding loop of Lys-49/Ser-49 sPLA₂s (9, 31,

32, 62), especially at positions 28, 32, and 33, are responsible for the lack of enzymatic activity of these sPLA₂ homologues.

Our results further indicate that, in AtnL, apart from the residues that take part in calcium binding, the rest of the substrate-binding and catalytic network has been well conserved, since relatively small changes in the molecule were enough to restore its long-lost enzymatic activity. The Lys-49/Ser-49 sPLA₂ homologues have lost their calcium-binding ability during evolution; therefore, it is conceivable that changes in the Ca²⁺-binding network other than that at position 49 would occur (32, 63). The conservation of the rest of the catalytic network could be a consequence of a lower frequency of mutations in Lys-49/Ser-49 myotoxins following acquisition of their particular function through accelerated evolution (63). Judging from their interfacial binding and kinetic properties, the LV and LW mutants are able to bind productively and with high affinity to membrane surfaces. The phospholipid molecule is subsequently well accommodated in the substrate-binding site, the tetrahedral intermediate is productively stabilized by the bound Ca²⁺ ion during turnover, and the products of catalysis are released from the active site. Therefore, the hypothesis that Lys-49 sPLA₂s are in fact active enzymes in which catalysis is interrupted at the stage of product release (36) seems highly unlikely in light of our results. Additionally, the overall enzymatic properties of the mutants are very similar to those of Atxs and to those of other group IIA sPLA₂s (44, 56), indicating that AtnL has retained all of the structural features important for enzymatic activity, apart from those involved in calcium coordination. This provides strong evidence that accommodation of a substrate molecule in the active site of Ser-49/Lys-49 sPLA₂ homologues is indeed possible, supporting the recently proposed connection between ligand binding and their mechanism of membrane damage (35–39).

Trp-31 Confers a Significant Advantage in Enzymatic Activity to the LW Mutant. Given the high degree of identity between AtnL and AtxA (74%) and the highly basic character of AtnL (with 23 basic residues and a net charge of +9), the preference of LW and LV for anionic phospholipids was expected (44). The activities of the mutants were identical, within experimental error, on pure anionic vesicles, which can be attributed to their high binding affinity for such membrane surfaces. Indeed, our SPR binding studies confirm that the binding affinities of LW, LV, and AtnL for POPG vesicles do not differ significantly and are higher than that

of AtxA, which is, in general, a very efficient sPLA₂. Under such high-affinity binding conditions, when most if not all the enzyme molecules in the assay mixture are bound to vesicles, the initial rates of hydrolysis are independent of the properties of the IBS of the sPLA₂ and the rates of hydrolysis reflect the effectiveness of the catalytic site. Therefore, the activities of the mutants on anionic vesicles indicate that their catalytic mechanisms operate with similar efficiency and that the residue at position 31 does not influence phospholipid binding to the active site or the catalytic reaction. It follows that the higher rates of hydrolysis by LW than by LV, observed on pure POPC and POPS/POPC vesicles, must be a consequence of higher membrane-binding affinity of the former, rather than catalytic site specificity. Indeed, according to our SPR binding experiments, there was a significant difference between the apparent interfacial binding affinity of LW and LV on POPC vesicles. On increasing the content of anionic phospholipid in PC vesicles, the dramatic 100-fold difference in activity between LW and LV, seen on pure POPC vesicles, was reduced only 2-fold, reflecting an increase in nonspecific electrostatic interactions (64), which mask the contribution of the amphiphilic Trp-31 that confers a significant advantage in interfacial binding affinity to the LW mutant when acting on PC-rich vesicles. The well-documented ability of a Trp residue on the IBS of sPLA₂s to have a major influence on their (patho)physiological roles (47, 52, 53, 55) is evident in the case of the LW mutant, whose efficiency in hydrolyzing PC-rich membranes is reflected in its high toxicity *in vivo* and *in vitro*. Indeed, the fact that the most striking differences in the properties of the LW and LV mutants are displayed both in their enzymatic activity on PC membranes and in toxicity *in vivo* strongly suggests that their mechanism(s) of toxic action depend(s) on their interfacial binding affinity and enzymatic activity on PC-rich target membranes.

AtnL Requires a Threshold Concentration of Anionic Phospholipid for Initiation of Its Membrane-Damaging Activity. The Ca²⁺-independent membrane-damaging activity is common to the Lys-49/Ser-49 sPLA₂ homologues, but the exact mechanism leading to disruption of the bilayer structure is unknown (11). In accordance with previous studies, our results indicate that the presence of a threshold concentration of anionic phospholipid in PC-rich membranes is required for Ca²⁺-independent membrane damage (18–20, 22). Indeed, AtnL, as well as LV and LW in the absence of calcium, was not able to induce calcein release from POPC or 10% POPG/POPC LUVs, notwithstanding their relatively high binding affinity for PC-rich vesicles and the high micromolar concentrations of protein used, but was highly effective when the amount of POPG was raised to 50%. This indicates that a threshold concentration of anionic POPG higher than 10% in the zwitterionic environment of POPC phospholipids is necessary for initiation of the Ca²⁺-independent mechanism of membrane damage. The lower threshold of phosphatidic acid (PA) required for induction of vesicle permeabilization, reported previously for natural AtnL (18), can be explained by the specific properties of this partially dianionic phospholipid, which is particularly well suited for the interfacial insertion of basic proteins (65). Significantly lower surface concentrations of PA than of PS in PC-rich vesicles were needed to enhance interfacial binding of sPLA₂s (64). Additionally, PA rendered egg yolk

PC vesicles more sensitive to the action of bothropstoxin I in comparison with the effect of the presence of PG at the same concentration (60). It is clear from our results that the presence of more than 10% POPG in zwitterionic POPC vesicles is required for initiating the membrane-damaging activity of AtnL; however, the threshold concentration of anionic phospholipid in other *in vitro* or *in vivo* systems will differ, depending on the specific nature of the phospholipid and the effective anionic charge density on the target membrane surface.

Restoration of Enzymatic Activity Affects the Membrane-Damaging Activity of AtnL in Multiple Ways. In contrast to AtnL, all the enzymatically active sPLA₂s tested, including LW and LV, induced calcein release from pure POPC as well as 10% POPG/POPC vesicles in a Ca²⁺-dependent manner. Their calcein release abilities correlated very well with their initial rates of hydrolysis, clearly indicating that enzymatic activity is responsible for vesicle disruption. Therefore, the phospholipolytic activity of LW and LV enables them to induce membrane damage at much lower concentrations of anionic phospholipid in the membrane than that necessary in the case of AtnL.

However, in the presence of 50% anionic phospholipid in POPC vesicles, LV and LW were unique among the enzymatically active sPLA₂s in their ability to disrupt vesicle integrity using a Ca²⁺-independent mechanism similar to that displayed by AtnL. The fact that calcium enhanced their calcein release capability suggests the contribution of enzymatic activity. However, AtnL was also more effective in the presence of calcium, indicating that the ion has an enhancing role in the mechanism of membrane structure disorganization even in the absence of enzymatic activity. In accordance with this, lysis of PS-enriched erythrocytes with myotoxin II, a Lys-49 sPLA₂, was significantly enhanced in the presence of calcium (22). However, regardless of the presence or absence of calcium, both mutants were less effective than AtnL in disrupting 50% POPG/POPC vesicles, indicating that a high proportion of anionic phospholipid in the membrane leads to protein–membrane interactions that are optimal for the Ca²⁺-independent membrane-damaging mechanism of AtnL. These interactions appear to be altered in the presence of calcium due to the hydrolytic ability of the mutants, which requires an orientation of the protein that is favorable for efficient and processive catalysis on the membrane surface, leading to a lower potency for membrane damage compared to that of AtnL. Indeed, the interactions of most Asp-49 sPLA₂s with the membrane surface are subtle and do not include a significant penetration or perturbation of the bilayer structure (4, 18, 19, 55), while AtnL and the Lys-49 myotoxin II from *Bothrops asper* induce a profound perturbation of the lipid chain arrangement in the membrane interior (18, 19). This is also in accordance with the perturbing action of AtnL and its mutants, but not AtxA, on immobilized POPG vesicles during our SPR measurements. Additionally, the fact that LW and LV also show lower potency than AtnL in the absence of calcium suggests that the mutations introduced in the Ca²⁺-binding loop and the active site of AtnL have somewhat impaired its Ca²⁺-independent membrane-damaging mechanism. Indeed, the evolutionary changes that have led to loss of enzymatic activity of AtnL, despite conserving most of the substrate-binding and catalytic network, appear

to have simultaneously optimized its membrane-damaging mechanism, which is likely to be affected by the reversal of these changes in the enzymatically active mutants of AtnL. This indicates that the substrate-binding pocket of AtnL has an active role in the process, which is in accordance with the recently proposed mechanism that couples ligand binding in the “active” site of Lys-49 sPLA₂s to specific conformational changes in the C-terminal region, which has long been associated with their membrane-damaging and myotoxic activity (11, 37). Crucial components of the proposed mechanism are Lys-122, which is conserved in Lys-49 sPLA₂s and forms a strong interaction with the peptide bond between Cys-29 and Gly-30 in the Ca²⁺-binding loop, and an exposed hydrophobic surface, which presumably perturbs the membrane and involves Phe-121 and Phe-124 in *Agkistrodon contortrix laticinctus* myotoxin (37). The role of Lys-122 could be performed by Arg-122 in AtnL, and the presence of Leu-121 and Phe-124 is also consistent with the model. Indeed, our preliminary crystallographic data suggest that Arg-122 in AtnL is oriented toward the Cys–Gly peptide bond, while Leu-121 and Phe-124 are exposed on the surface of the molecule (D. Turk, personal communication). On the contrary, position 122 is occupied by the negatively charged Asp in Atxs, which, despite their high level of sequence similarity with AtnL, do not display a Ca²⁺-independent membrane-damaging mechanism. Thus, the mutations introduced in AtnL that restore its enzymatic activity have affected its Ca²⁺-independent membrane-damaging mechanism by simultaneously providing the interactions with the membrane surface necessary for enzymatic activity in the presence of calcium and by altering the optimal interactions with a single phospholipid molecule in its substrate-binding pocket that are necessary for its Ca²⁺-independent mechanism, even in the absence of calcium.

The results presented in this study clear the road for differentiation between the mechanisms of membrane damage displayed by the nonmyotoxic Atxs on one hand and AtnL on the other. AtnL disrupts vesicle membrane integrity in a noncooperative manner that leads to release of the aqueous content and includes significant perturbation of the bilayer interior, as stated above, resulting in vesicle/phospholipid structures with slightly increased average sizes (Figure 4), most probably resulting from binding and incorporation of AtnL molecules in the membrane. Although the process includes formation of small amounts of larger phospholipid structures, the latter reflects aggregation rather than fusion of vesicles. This was confirmed by our FRET studies, since lipid mixing was detected solely in the case of the enzymatically active sPLA₂s, including LW and LV, and only in the presence of calcium, pointing to the fact that membrane fusion is a consequence of enzymatic activity, as seen in the well-known fusogenic properties of the products of phospholipolysis (66–68). Indeed, incubation of 50% POPG/POPC vesicles with the enzymatically active AtxA and LW caused phospholipid structural rearrangements characteristic of vesicle fusion. The extensive calcein dequenching, detected with the enzymatically active Atxs exclusively in the presence of calcium, is therefore a consequence of leakage of the vesicle contents that accompanies the fusion events and/or occurs during collapse of large fused vesicles (69). Results of electron microscopy and NMR studies obtained after treatment of dipalmitoyl-

PC LUVs with enzymatically active sPLA₂ have revealed profound changes in vesicle morphology, leading to the appearance of a heterogeneous mix of mostly lamellar phospholipid structures, including fusion-generated large vesicular structures (66, 70). In agreement with the observations of Burack et al. (66, 70), some of the phospholipid structures resulting from treatment of vesicles with enzymatically active sPLA₂s were similar in size to the original vesicles, which is in accordance with the fact that not all the calcein was released from the vesicles, and that complete lipid mixing was never observed. Thus, while the Ca²⁺-independent membrane damage by AtnL is characterized by a disruption of vesicle integrity that does not involve membrane fusion, LV and LW are able to act in a manner similar to that of Atxs in the presence of calcium, where vesicle fusion is dependent on enzymatic activity and is accompanied by leakage of the contents. Since LW and LV also cause vesicle disruption in the absence of calcium, unlike AtxA but similarly to AtnL, they are able to utilize both mechanisms of membrane damage, depending on the calcium concentration available and the surface concentration of anionic phospholipids. It is evident that, with their acquired enzymatic activity, the mutants of AtnL have expanded their potential for inducing membrane structural changes and damage, since they have the ability to use both the Ca²⁺-dependent and Ca²⁺-independent mechanisms.

Cytotoxicity. In vitro cell culture studies have shown that high concentrations of sPLA₂ myotoxins exert a potent cytolytic activity on a broad range of cells (9, 16, 21, 27). The primary cause of cytotoxicity in vitro and myotoxicity in vivo, displayed by the Lys-49/Ser-49 sPLA₂s, is most probably a perturbation of the structural integrity of the plasma membrane (11, 14, 18, 20–22). The fact that the highly specific and potent presynaptically acting neurotoxic AtxA displays the highest cytotoxic potency toward C2C12 myoblasts suggests a nonspecific action on the PC-rich plasma membrane, most probably connected to its high level of enzymatic activity (44). Indeed, the cytotoxicity of AtxA, LW, LV, and AtnL correlated well with their phospholipolytic and calcein release efficiency on pure POPC and 10% POPG/POPC vesicles, indicating that enzymatic activity plays a crucial role in myoblast damage. In addition, the ability of LW and LV to damage the PC-rich plasma membrane of C2C12 myoblasts is consistent with their Ca²⁺-dependent calcein-releasing action on PC-rich vesicles that contain low concentrations of anionic lipid. Accordingly, AtnL, which requires a critical, higher surface concentration of anionic lipid to effectively permeabilize PC-rich vesicles, was very weak in inducing cytotoxicity in C2C12 myoblasts, as well as in L-6 myoblasts (16). The significantly higher cytotoxic potency of AtnL toward C2C12 myotubes than that determined on undifferentiated cells is consistent with its specific targeting of differentiated muscle fibers in vivo (17) and in vitro (16). Also, differentiated C2C12 cells have been shown to be much more sensitive to the specific action of a range of Lys-49 and Asp-49 sPLA₂ myotoxins, but not to other general membrane-perturbing agents (59). The higher sensitivity of differentiated muscle cells to sPLA₂ myotoxins has been suggested to be a consequence of some specific changes in the membrane composition or structure occurring during the differentiation process (17, 59). Interestingly, it has been shown recently that transient exposure of PS on

the surface of differentiating C2C12 myoblasts is crucial in the process of fusion and differentiation (71). An increase in the surface concentration of anionic phospholipids in the sarcolemma would enhance interfacial binding of all basic sPLA₂s, thus inducing the Ca²⁺-independent membrane-damaging mechanism of AtnL, LW, and LV, but simultaneously enabling a higher extent of phospholipolysis by the enzymatically active Atns, as well as by LW and LV. In accordance with this, the cytotoxic potency of AtnL and the enzymatically active sPLA₂s on C2C12 myotubes was considerably higher and showed a lower level of variability than on myoblasts. Thus, the relatively potent enzymatic activity displayed by LW on PC-rich membranes has increased its cytotoxic potency relative to that of AtnL and LV on C2C12 cells, which is consistent with its higher lethality in vivo. However, the ability of LW to effectively damage C2C12 myoblasts, in contrast to AtnL but similarly to AtnA, suggests that enzymatic activity has broadened the specificity of its membrane-damaging and (cyto)toxic action. This opens up the possibility that the increase in lethality of the LW mutant is not necessarily dependent solely on its specific myotoxic action, but also on some additional toxic activity, which could have been activated by the introduction of enzymatic activity. This question requires further study and is under current investigation in our laboratory.

The results of the present study indicate that Lys-49/Ser-49 sPLA₂ myotoxins have evolved in the direction of loss of Ca²⁺-binding ability and enzymatic activity under selective pressure to optimize their Ca²⁺-independent membrane-damaging mechanism and to increase the specificity of their myotoxic action. This has been achieved through subtle changes of calcium-binding residues without affecting the rest of the catalytic network, strongly implying that binding a phospholipid molecule in their inactive catalytic center has an important role in the process of membrane damage. Although the restoration of enzymatic activity of AtnL increased its cytotoxic potency and lethality in general, it had a negative effect on its Ca²⁺-independent mechanism of membrane damage and on its specific targeting of differentiated muscle cells in vitro. The latter supports the idea of an evolutionary specialization of Ser-49/Lys-49 sPLA₂s to perform the role of abundant and weakly lethal, but specific-muscle-targeting, toxins in the ensemble of pharmacologically active molecules found in snake venom.

ACKNOWLEDGMENT

We are grateful to Zala Jenko Pražnikar for preparation of recombinant AtnL and determination of its toxicity, Dr. David C. Wilton for kindly providing the expression plasmid encoding rat liver fatty acid-binding protein, Dr. Angelo Poletti for providing the mouse myoblast C2C12 cell line, Dr. Gregor Anderluh and Andrej Bavdek for help in the SPR experiments, Dr. Tadej Malovrh for help in the lethality measurements, Dr. Bogdan Kralj for molecular mass analysis, and Dr. Roger H. Pain for critical reading of the manuscript.

REFERENCES

- Schaloske, R. H., and Dennis, E. A. (2006) The phospholipase A₂ superfamily and its group numbering system, *Biochim. Biophys. Acta* 1761, 1246–1259.
- Kini, R. M. (2003) Excitement ahead: structure, function and mechanism of snake venom phospholipase A₂ enzymes, *Toxicon* 42, 827–840.
- Kudo, I., and Murakami, M. (2002) Phospholipase A₂ enzymes, *Prostaglandins Other Lipid Mediat.* 68–69, 3–58.
- Berg, O. G., Gelb, M. H., Tsai, M. D., and Jain, M. K. (2001) Interfacial enzymology: the secreted phospholipase A₂-paradigm, *Chem. Rev.* 101, 2613–2654.
- Scott, D. L., White, S. P., Otwinowski, Z., Yuan, W., Gelb, M. H., and Sigler, P. B. (1990) Interfacial catalysis: the mechanism of phospholipase A₂, *Science* 250, 1541–1546.
- Yu, B. Z., Rogers, J., Nicol, G. R., Theopold, K. H., Seshadri, K., Vishweshwara, S., and Jain, M. K. (1998) Catalytic significance of the specificity of divalent cations as K_s^{*} and k_{cat}^{*} cofactors for secreted phospholipase A₂, *Biochemistry* 37, 12576–12587.
- Yu, B. Z., Berg, O. G., and Jain, M. K. (1993) The divalent cation is obligatory for the binding of ligands to the catalytic site of secreted phospholipase A₂, *Biochemistry* 32, 6485–6492.
- Pungerčar, J., Liang, N. S., Strukelj, B., and Gubenšek, F. (1990) Nucleotide sequence of a cDNA encoding ammodytin L, *Nucleic Acids Res.* 18, 4601.
- Križaj, I., Bieber, A. L., Ritonja, A., and Gubenšek, F. (1991) The primary structure of ammodytin L, a myotoxic phospholipase A₂ homologue from *Vipera ammodytes* venom, *Eur. J. Biochem.* 202, 1165–1168.
- Polgár, J., Magnenat, E. M., Peitsch, M. C., Wells, T. N., and Clemetson, K. J. (1996) Asp-49 is not an absolute prerequisite for the enzymic activity of low-M_r phospholipases A₂: purification, characterization and computer modelling of an enzymically active Ser-49 phospholipase A₂, ecarpholin S, from the venom of *Echis carinatus sochureki* (saw-scaled viper), *Biochem. J.* 319, 961–968.
- Lomonte, B., Angulo, Y., and Calderón, L. (2003) An overview of lysine-49 phospholipase A₂ myotoxins from crotalid snake venoms and their structural determinants of myotoxic action, *Toxicon* 42, 885–901.
- van den Bergh, C. J., Slotboom, A. J., Verheij, H. M., and de Haas, G. H. (1988) The role of aspartic acid-49 in the active site of phospholipase A₂. A site-specific mutagenesis study of porcine pancreatic phospholipase A₂ and the rationale of the enzymatic activity of [lysine49]phospholipase A₂ from *Agkistrodon piscivorus piscivorus* venom, *Eur. J. Biochem.* 176, 353–357.
- Scott, D. L., Achari, A., Vidal, J. C., and Sigler, P. B. (1992) Crystallographic and biochemical studies of the (inactive) Lys-49 phospholipase A₂ from the venom of *Agkistrodon piscivorus piscivorus*, *J. Biol. Chem.* 267, 22645–22657.
- Gutiérrez, J. M., and Ownby, C. L. (2003) Skeletal muscle degeneration induced by venom phospholipases A₂: insights into the mechanisms of local and systemic myotoxicity, *Toxicon* 42, 915–931.
- Thouin, L. G., Ritonja, A., Gubenšek, F., and Russell, F. E. (1982) Neuromuscular and lethal effects of phospholipase A from *Vipera ammodytes* venom, *Toxicon* 20, 1051–1058.
- Incerpi, S., de Vito, P., Luly, P., and Rufini, S. (1995) Effect of ammodytin L from *Vipera ammodytes* on L-6 cells from rat skeletal muscle, *Biochim. Biophys. Acta* 1268, 137–142.
- Bernardini, S., Cannata, S., Filoni, S., Luly, P., and Rufini, S. (1996) Effect of ammodytin L from the venom of *Vipera ammodytes* on *Xenopus laevis* differentiated muscle fibres and regenerating limbs, *Toxicon* 34, 81–90.
- Rufini, S., Cesaroni, P., Desideri, A., Farias, R., Gubenšek, F., Gutiérrez, J. M., Luly, P., Massoud, R., Morero, R., and Pedersen, J. Z. (1992) Calcium ion independent membrane leakage induced by phospholipase-like myotoxins, *Biochemistry* 31, 12424–12430.
- Pedersen, J. Z., de Arcuri, B. F., Morero, R. D., and Rufini, S. (1994) Phospholipase-like myotoxins induce rapid membrane leakage of non-hydrolyzable ether-lipid liposomes, *Biochim. Biophys. Acta* 1190, 177–180.
- Díaz, C., Gutiérrez, J. M., Lomonte, B., and Gené, J. A. (1991) The effect of myotoxins isolated from Bothrops snake venoms on multilamellar liposomes: relationship to phospholipase A₂, anticoagulant and myotoxic activities, *Biochim. Biophys. Acta* 1070, 455–460.
- Lomonte, B., Tarkowski, A., and Hanson, L. A. (1994) Broad cytolytic specificity of myotoxin II, a lysine-49 phospholipase A₂ of *Bothrops asper* snake venom, *Toxicon* 32, 1359–1369.
- Díaz, C., León, G., Rucavado, A., Rojas, N., Schroit, A. J., and Gutiérrez, J. M. (2001) Modulation of the susceptibility of human erythrocytes to snake venom myotoxic phospholipases A₂: role of negatively charged phospholipids as potential membrane binding sites, *Arch. Biochem. Biophys.* 391, 56–64.

23. Križaj, I., and Gubenšek, F. (2000) Neuronal receptors for phospholipases A₂ and β-neurotoxicity, *Biochimie* 82, 807–814.
24. Rigoni, M., Caccin, P., Gschmeissner, S., Koster, G., Postle, A. D., Rossetto, O., Schiavo, G., and Montecucco, C. (2005) Equivalent effects of snake PLA₂ neurotoxins and lysophospholipid-fatty acid mixtures, *Science* 310, 1678–1680.
25. Caccin, P., Rigoni, M., Bisceglie, A., Rossetto, O., and Montecucco, C. (2006) Reversible skeletal neuromuscular paralysis induced by different lysophospholipids, *FEBS Lett.* 580, 6317–6321.
26. Rigoni, M., Pizzo, P., Schiavo, G., Weston, A. E., Zatti, G., Caccin, P., Rossetto, O., Pozzan, T., and Montecucco, C. (2007) Calcium influx and mitochondrial alterations at synapses exposed to snake neurotoxins or their phospholipid hydrolysis products, *J. Biol. Chem.* 282, 11238–11245.
27. Bultrón, E., Gutiérrez, J. M., and Thelestam, M. (1993) Effects of *Bothrops asper* (terciopelo) myotoxin III, a basic phospholipase A₂, on liposomes and mouse gastrocnemius muscle, *Toxicon* 31, 217–222.
28. Soares, A. M., Andrião-Escarso, S. H., Bortoleto, R. K., Rodrigues-Simioni, L., Arni, R. K., Ward, R. J., Gutiérrez, J. M., and Giglio, J. R. (2001) Dissociation of enzymatic and pharmacological properties of piratoxins-I and -III, two myotoxic phospholipases A₂ from *Bothrops pirajai* snake venom, *Arch. Biochem. Biophys.* 387, 188–196.
29. Shimohigashi, Y., Tani, A., Matsumoto, H., Nakashima, K., and Yamaguchi, Y. (1995) Lysine-49-phospholipases A₂ from *Trimeresurus flavoviridis* venom are membrane-acting enzymes, *J. Biochem. (Tokyo)* 118, 1037–1044.
30. Yamaguchi, Y., Shimohigashi, Y., Chiwata, T., Tani, A., Chijiwa, T., Lomonte, B., and Ohno, M. (1997) Lys-49-phospholipases A₂ as active enzyme for β-arachidonoyl phospholipid bilayer membranes, *Biochem. Mol. Biol. Int.* 43, 19–26.
31. Ward, R. J., Chioato, L., de Oliveira, A. H. C., Ruller, R., and Sá, J. M. (2002) Active-site mutagenesis of a Lys49-phospholipase A₂: biological and membrane-disrupting activities in the absence of catalysis, *Biochem. J.* 362, 89–96.
32. van den Bergh, C. J., Slotboom, A. J., Verheij, H. M., and de Haas, G. H. (1989) The role of Asp-49 and other conserved amino acids in phospholipases A₂ and their importance for enzymatic activity, *J. Cell. Biochem.* 39, 379–390.
33. Holland, D. R., Clancy, L. L., Muchmore, S. W., Ryde, T. J., Einspahr, H. M., Finzel, B. C., Heinrikson, R. L., and Watenpugh, K. D. (1990) The crystal structure of a lysine 49 phospholipase A₂ from the venom of the cottonmouth snake at 2.0-Å resolution, *J. Biol. Chem.* 265, 17649–17656.
34. Li, Y., Yu, B. Z., Zhu, H., Jain, M. K., and Tsai, M. D. (1994) Phospholipase A₂ engineering. Structural and functional roles of the highly conserved active site residue aspartate-49, *Biochemistry* 33, 14714–14722.
35. Pedersen, J. Z., Lomonte, B., Massoud, R., Gubenšek, F., Gutiérrez, J. M., and Rufini, S. (1995) Autocatalytic acylation of phospholipase-like myotoxins, *Biochemistry* 34, 4670–4675.
36. Lee, W. H., da Silva Giotto, M. T., Marangoni, S., Toyama, M. H., Polikarpov, I., and Garratt, R. C. (2001) Structural basis for low catalytic activity in Lys49 phospholipases A₂—a hypothesis: the crystal structure of piratoxin II complexed to fatty acid, *Biochemistry* 40, 28–36.
37. Ambrosio, A. L. B., Nonato, M. C., de Araújo, H. S. S., Arni, R., Ward, R. J., Ownby, C. L., de Souza, D. H. F., and Garratt, R. C. (2005) A molecular mechanism for Lys49-phospholipase A₂ activity based on ligand-induced conformational change, *J. Biol. Chem.* 280, 7326–7335.
38. Watanabe, L., Soares, A. M., Ward, R. J., Fontes, M. R. M., and Arni, R. K. (2005) Structural insights for fatty acid binding in a Lys49-phospholipase A₂: crystal structure of myotoxin II from *Bothrops moojeni* complexed with stearic acid, *Biochimie* 87, 161–167.
39. Murakami, M. T., Viçoti, M. M., Abrego, J. R. B., Lourenzoni, M. R., Cintra, A. C. O., Arruda, E. Z., Tomaz, M. A., Melo, P. A., and Arni, R. K. (2007) Interfacial surface charge and free accessibility to the PLA₂-active site-like region are essential requirements for the activity of Lys49 PLA₂ homologues, *Toxicon* 49, 378–387.
40. Sá, J. M., Chioato, L., Ferreira, T. L., De Oliveira, A. H. C., Ruller, R., Rosa, J. C., Greene, L. J., and Ward, R. J. (2004) Topology of the substrate-binding site of a Lys49-phospholipase A₂ influences Ca²⁺-independent membrane-damaging activity, *Biochem. J.* 382, 191–198.
41. Križaj, I., Liang, N. S., Pungerčar, J., Štrukelj, B., Ritonja, A., and Gubenšek, F. (1992) Amino acid and cDNA sequences of a neutral phospholipase A₂ from the long-nosed viper (*Vipera ammodytes ammodytes*) venom, *Eur. J. Biochem.* 204, 1057–1062.
42. Worrall, A. F., Evans, C., and Wilton, D. C. (1991) Synthesis of a gene for rat liver fatty-acid-binding protein and its expression in *Escherichia coli*, *Biochem. J.* 278, 365–368.
43. Pungerčar, J., Križaj, I., Liang, N. S., and Gubenšek, F. (1999) An aromatic, but not a basic, residue is involved in the toxicity of group-II phospholipase A₂ neurotoxins, *Biochem. J.* 341, 139–145.
44. Petan, T., Križaj, I., Gelb, M. H., and Pungerčar, J. (2005) Ammodytoxins, potent presynaptic neurotoxins, are also highly efficient phospholipase A₂ enzymes, *Biochemistry* 44, 12535–12545.
45. Petan, T., Križaj, I., Gubenšek, F., and Pungerčar, J. (2002) Phenylalanine-24 in the N-terminal region of ammodytoxins is important for both enzymic activity and presynaptic toxicity, *Biochem. J.* 363, 353–358.
46. Radvanyi, F., Jordan, L., Russo-Marie, F., and Bon, C. (1989) A sensitive and continuous fluorometric assay for phospholipase A₂ using pyrene-labeled phospholipids in the presence of serum albumin, *Anal. Biochem.* 177, 103–109.
47. Bezzine, S., Koduri, R. S., Valentin, E., Murakami, M., Kudo, I., Ghomashchi, F., Sadilek, M., Lambeau, G., and Gelb, M. H. (2000) Exogenously added human group X secreted phospholipase A₂ but not the group IB, IIA, and V enzymes efficiently release arachidonic acid from adherent mammalian cells, *J. Biol. Chem.* 275, 3179–3191.
48. Struck, D. K., Hoekstra, D., and Pagano, R. E. (1981) Use of resonance energy transfer to monitor membrane fusion, *Biochemistry* 20, 4093–4099.
49. Anderluh, G., Beseničar, M., Kladnik, A., Lakey, J. H., and Maček, P. (2005) Properties of nonfused liposomes immobilized on an L1 Biacore chip and their permeabilization by a eukaryotic pore-forming toxin, *Anal. Biochem.* 344, 43–52.
50. Reed, L. J., and Muench, H. (1938) A simple method of estimating fifty per cent endpoints, *Am. J. Hygiene* 27, 493–497.
51. Pungerčar, J., Vučemilo, N., Faure, G., Bon, C., Verheij, H. M., Gubenšek, F., and Križaj, I. (1998) Ammodytin L, an inactive phospholipase A₂ homologue with myotoxicity in mice, binds to the presynaptic acceptor of the beta-neurotoxic ammodytoxin C in Torpedo: an indication for a phospholipase A₂ activity-independent mechanism of action of beta-neurotoxins in fish? *Biochem. Biophys. Res. Commun.* 244, 514–518.
52. Han, S. K., Kim, K. P., Koduri, R., Bittova, L., Munoz, N. M., Leff, A. R., Wilton, D. C., Gelb, M. H., and Cho, W. (1999) Roles of Trp31 in high membrane binding and proinflammatory activity of human group V phospholipase A₂, *J. Biol. Chem.* 274, 11881–11888.
53. Beers, S. A., Buckland, A. G., Giles, N., Gelb, M. H., and Wilton, D. C. (2003) Effect of tryptophan insertions on the properties of the human group IIA phospholipase A₂: mutagenesis produces an enzyme with characteristics similar to those of the human group V phospholipase A₂, *Biochemistry* 42, 7326–7338.
54. Ivanovski, G., Petan, T., Križaj, I., Gelb, M. H., Gubenšek, F., and Pungerčar, J. (2004) Basic amino acid residues in the β-structure region contribute, but not critically, to presynaptic neurotoxicity of ammodytoxin A, *Biochim. Biophys. Acta* 1702, 217–225.
55. Bezzine, S., Bollinger, J. G., Singer, A. G., Veatch, S. L., Keller, S. L., and Gelb, M. H. (2002) On the binding preference of human groups IIA and X phospholipases A₂ for membranes with anionic phospholipids, *J. Biol. Chem.* 277, 48523–48534.
56. Singer, A. G., Ghomashchi, F., Le Calvez, C., Bollinger, J., Bezzine, S., Rouault, M., Sadilek, M., Nguyen, E., Lazdunski, M., Lambeau, G., and Gelb, M. H. (2002) Interfacial kinetic and binding properties of the complete set of human and mouse groups I, II, V, X, and XII secreted phospholipases A₂, *J. Biol. Chem.* 277, 48535–48549.
57. Kayalar, C., and Düzgüneş, N. (1986) Membrane action of colicin E1: detection by the release of carboxyfluorescein and calcein from liposomes, *Biochim. Biophys. Acta* 860, 51–56.
58. Stahelin, R. V., and Cho, W. (2001) Differential roles of ionic, aliphatic, and aromatic residues in membrane-protein interactions: a surface plasmon resonance study on phospholipases A₂, *Biochemistry* 40, 4672–4678.

59. Angulo, Y., and Lomonte, B. (2005) Differential susceptibility of C2C12 myoblasts and myotubes to group II phospholipase A₂ myotoxins from crotalid snake venoms, *Cell Biochem. Funct.* **23**, 307–313.
60. Chioato, L., Aragão, E. A., Lopes Ferreira, T., Ivo de Medeiros, A., Faccioli, L. H., and Ward, R. J. (2007) Mapping of the structural determinants of artificial and biological membrane damaging activities of a Lys49 phospholipase A₂ by scanning alanine mutagenesis, *Biochim. Biophys. Acta* **1768**, 1247–1257.
61. Mora, R., Valverde, B., Díaz, C., Lomonte, B., and Gutiérrez, J. M. (2005) A Lys49 phospholipase A₂ homologue from *Bothrops asper* snake venom induces proliferation, apoptosis and necrosis in a lymphoblastoid cell line, *Toxicon* **45**, 651–660.
62. Ward, R. J., Alves, A. R., Ruggiero Neto, J., Arni, R. K., and Casari, G. (1998) A SequenceSpace analysis of Lys49 phospholipases A₂: clues towards identification of residues involved in a novel mechanism of membrane damage and in myotoxicity, *Protein Eng.* **11**, 285–294.
63. Ohno, M., Chijiwa, T., Oda-Ueda, N., Ogawa, T., and Hattori, S. (2003) Molecular evolution of myotoxic phospholipases A₂ from snake venom, *Toxicon* **42**, 841–854.
64. Buckland, A. G., and Wilton, D. C. (2000) Anionic phospholipids, interfacial binding and the regulation of cell functions, *Biochim. Biophys. Acta* **1483**, 199–216.
65. Kooijman, E. E., Tieleman, D. P., Testerink, C., Munnik, T., Rijkers, D. T., Burger, K. N., and de Kruijff, B. (2007) An electrostatic/hydrogen bond switch as the basis for the specific interaction of phosphatidic acid with proteins, *J. Biol. Chem.* **282**, 11356–11364.
66. Burack, W. R., Dibble, A. R., Allietta, M. M., and Biltonen, R. L. (1997) Changes in vesicle morphology induced by lateral phase separation modulate phospholipase A₂ activity, *Biochemistry* **36**, 10551–10557.
67. Davidsen, J., Mouritsen, O. G., and Jørgensen, K. (2002) Synergistic permeability enhancing effect of lysophospholipids and fatty acids on lipid membranes, *Biochim. Biophys. Acta* **1564**, 256–262.
68. Brown, W. J., Chambers, K., and Doody, A. (2003) Phospholipase A₂ (PLA₂) enzymes in membrane trafficking: mediators of membrane shape and function, *Traffic* **4**, 214–221.
69. Morris, S. J., Gibson, C. C., Smith, P. D., Greif, P. C., Stirk, C. W., Bradley, D., Haynes, D. H., and Blumenthal, R. (1985) Rapid kinetics of Ca²⁺-induced fusion of phosphatidylserine/phosphatidylethanolamine vesicles. The effect of bilayer curvature on leakage, *J. Biol. Chem.* **260**, 4122–4127.
70. Burack, W. R., Yuan, Q., and Biltonen, R. L. (1993) Role of lateral phase separation in the modulation of phospholipase A₂ activity, *Biochemistry* **32**, 583–589.
71. van den Eijnde, S. M., van den Hoff, M. J., Reutelingsperger, C. P., van Heerde, W. L., Henfling, M. E., Vermeij-Keers, C., Schutte, B., Borgers, M., and Ramaekers, F. C. (2001) Transient expression of phosphatidylserine at cell-cell contact areas is required for myotube formation, *J. Cell Sci.* **114**, 3631–3642.

BI701304E